Accepted Manuscript

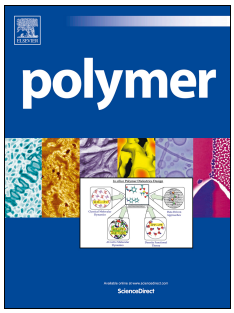

RAFT-mediated emulsion polymerization of styrene with a thermoresponsive MacroCTA

Clovia I. Holdsworth, Zhongfan Jia, Michael J. Monteiro

PII: S0032-3861(16)30788-1

DOI: 10.1016/j.polymer.2016.08.108

Reference: JPOL 19005

To appear in: *Polymer*

Received Date: 26 July 2016

Revised Date: 29 August 2016

Accepted Date: 31 August 2016

Please cite this article as: Holdsworth CI, Jia Z, Monteiro MJ, RAFT-mediated emulsion polymerization of styrene with a thermoresponsive MacroCTA, *Polymer* (2016), doi: 10.1016/j.polymer.2016.08.108.

RAFT-Mediated Emulsion polymerization of Styrene with a Thermoresponsive MacroCTA.

*Clovia I. Holdsworth,[2] Zhongfan Jia,[1] and Michael J. Monteiro[1,]**

1. Australian Institute for Bioengineering and Nanotechnology, The University of Queensland, Brisbane QLD 4072, Australia

2. Discipline of Chemistry, School of Environmental and Life Sciences, The University of Newcastle, Callaghan, NSW 2308, Australia

*author to whom correspondence should be sent:

e-mail: m.monteiro@uq.edu.au

ABSTRACT

Heterogeneous RAFT polymerization is an attractive ‘living’ radical polymerization technique to control not only the molecular weight distribution but also the particles size distribution. Here, we demonstrate the use of a thermoresponsive RAFT macro chain transfer agent (MacroCTA) to form seed particles for the chain extension of styrene to form block copolymer latex particles. By incorporating a few styrene units into the MacroCTA, the polymerizations become faster, producing both narrow particle size and molecular weight distribution. This is due to the ‘superswelling effect’, in which all the seed particles swell with monomer and nucleated at the same time. The resulting latex particles could then be transformed into a variety of nanostructures by cooling below the lower critical solution temperature of the thermoresponsive block in the presence of a plasticizer for polystyrene. The dominant structure was cylindrical worms with the observation of other structures including jelly fish and the rare disc. Cooling under ultrasound produced either vesicles or cauliflower structures. The work demonstrated that utilizing the ‘superswelling effect’, control over the rate, and molecular weight and particle size distributions could be obtained, providing design parameters to construct new nanostructures.

INTRODUCTION

The implementation of reversible addition-fragmentation chain transfer (RAFT) in heterogeneous polymerizations has progressed over the past 16 years.[1-8] Heterogeneous RAFT polymerization would seem to be the most attractive to industry compared with other 'living' radical polymerization techniques due to ease of implementation.[1, 8] All that would be required is the substitution of conventional chain transfer agents with that of RAFT agents without a change in reactor design or reaction conditions. Further support for this advantage is through kinetic simulations of bulk or solution RAFT-mediated polymerizations that importantly show the rate of RAFT polymerization is similar to polymerizations in the absence of RAFT agent.[9, 10] The only difference results from high glass transition polymers where the onset of the gel affect will be deferred to higher conversions due to chain length dependent termination.[11, 12] The initial work into RAFT-mediated emulsion polymerization demonstrated a major limitation due to the lack of colloidal stability and a resultant small red-monomer layer, suggesting that RAFT agent transportation was problematic.[1] The most probable reason for emulsion instability came from elegant work by Schork and coworkers[13], who showed that the 'superswelling effect' has the capability to significant swell micelles early in the polymerization, leading to a catastrophic destabilization.

Many methods have successfully overcome this problem, including multi-step procedures,[14, 15] surfactant-like RAFT agents,[16-18] miniemulsions,[19-21], seeded,[22] and ab initio[23-27]. Our group used an alternative approach of using thermoresponsive nanoreactors to overcome this issue, in which a poly(N-isopropylacrylamide) (PNIPAM) RAFT macro-chain transfer agent (MacroCTA) was mixed with a diblock copolymer consisting of PNIPAM and poly(dimethylacrylamide) to form stable seed particles.[28, 29] The chain extension of styrene led to excellent control over the molecular weight distribution (MWD) and particle size distribution (PSD). This approach allowed spherical particles to be dialed-up to a desired

diameter and with a desired narrow MWD, an advance on previous techniques. The technique formed the basis of the *in situ* driven self-assembly directly after polymerization to produce a variety of nanostructures in water (see below).

The most recent advance in dispersion polymerizations using RAFT is the *in situ* polymerization and self-assembly of nanostructures directly in water. Two techniques have been found to be highly versatile and can be carried out at high weight fractions of polymer in water (> 10 wt%). The first method, polymerization induced self-assembly (PISA), uses a water-soluble RAFT macro-chain transfer agent (MacroCTA) that when extended with a hydrophobic monomer self-assembles into spheres, worms, lamellae, jellyfish, yolk-shell, onion-like micelles and vesicles.[30] The second method developed by our group[31-33] involves the use a thermoresponsive RAFT MacroCTA that form seed particles stabilized by surfactant above its lower critical solution temperature (LCST). The MacroCTA is chain extended with monomer to form block copolymers within these particles, and a wide range of nanostructures formed when decreasing the temperature of the latex below the LCST (denoted as the temperature directed morphology transformation (TDMT) method). These include spheres, donuts, worms, rods, and vesicles.[31, 32] The advantage of our method is that multiple types of functionality can be introduced via the MacroCTAs onto the surface of these nanostructures for orthogonal coupling to polymers and biomolecules.[34] Additionally, the structures can be freeze-dried and then rehydrated without altering the original nanostructure.

Our method has recently been used to create a unique and stable tadpole structure by combining two PNIPAM MacroCTAs; one with a high LCST and the other with a low LCST that were chain extended with styrene.[35] By decreasing the temperature between that of the two LCSTs, the block with the high LCST formed the tail and the block with the low LCST formed the head. Not only was a narrow MWD produced, but interestingly, the PSD was also

narrow. We postulated that this could be due to the one or two styrene units incorporated into the MacroCTA, resulting in not only lowering the LCST[36-38] but acting as a superswelling agent for monomer into the PNIPAM seed particles[28]. It was found that when a few styrene units were incorporated into the PNIPAM chain, there was a 6-fold increase in the swelling volume compared to that for high molecular weight polystyrene.[28] In this work, we wanted to gain a greater understanding of the effects of incorporating styrene units into the PNIPAM MacroCTA on the polymerization kinetics, MWD and PSD using different monomer to MacroCTA feed ratios. We also wanted to determine whether this had an effect on the nanostructure formation upon direct cooling to 25 ^{o}C or sonication and then cooling to 25 ^{o}C.

EXPERIMENTAL

Materials

All reagents and solvents were of analytical grade and used as received unless otherwise stated, these included: dichloromethane (DCM; Aldrich AR grade), dimethylsulfoxide (DMSO; Aldrich, AR grade) and tetrahydrofuran (THF; Labscan, HPLC grade). Styrene was passed through a column of basic alumina (activity I) to remove inhibitor. N-isopropylacrylamide was recrystallised twice from hexane prior to use. Azobisisobutyronitrile (AIBN) and 1,1′-Azobis(cyanocyclohexane) (Vazo88) were recrystallized twice from methanol prior to use. MilliQ Water (18.2 MΩcm^{-1}) was generated using a Millipore MilliQ-Academic Water Purification System.

Synthesis of Statistical Poly(N-isopropylacrylamide-co-styrene)-SC(=S)SC$_4$H$_9$ MacroCTA.

(i) Synthesis of Poly(NIPAM$_{32}$-co-STY$_{1.33}$)-SC(=S)SC$_4$H$_9$ MacroCTA1

The chain transfer agent (CTA, methyl 2-(butylthiocarbonothioylthio)propanoate) was synthesized according to ref[28].

N-isopropylacrylamide (NIPAM, 2.427 g, 0.0214 mol, 97.5 mol% feed) and styrene (STY, 0.0572 g, 5.50 x 10^{-4} mol, 2.5 mol% feed), AIBN (0.0012 g, 7.3 x 10^{-6} mol), CTA (0.134 g, 5.3 x 10^{-4} mol) and DMSO (5 mL) were placed in a Schlenk tube equipped with a magnetic stirrer bar. The reaction mixture was purged with argon for 20 min, then heated at 65^{o}C for 18 hours. The reaction mixture was cooled, diluted with DCM and washed 3-times with brine. The DCM layers were dried over anhydrous $MgSO_4$, filtered and reduced in volume by rotary evaporation. The polymer was recovered by precipitation into petroleum ether, followed by filtration and drying under vacuum for 24 h at 25 °C.

The conversion was 76 % as determined from ^{1}H NMR spectroscopy. The amount of styrene in the resulting copolymer ***P(NIPAM$_{32}$-co-STY$_{1.33}$)-SC(=S)SC$_4$H$_9$ – MacroCTA1*** ($M_{n,SEC}$= 3800, PDI = 1.07, $M_{n,NMR}$ = 4000) was found to be 4 %, which is correlating to 1 STY unit per 24 NIPAM units.

(ii) Synthesis of Poly(NIPAM$_{30}$-co-STY$_{2.50}$)-SC(=S)SC$_4$H$_9$ MacroCTA2

N-isopropylacrylamide (NIPAM, 2.360 g, 0.00209 mol, 95 mol% feed) and styrene (STY, 0.114 g, 0.00110 mol, 5 mol% feed), AIBN (0.0012 g, 7.3 x 10^{-6} mol), CTA (0.134 g, 5.3 x 10^{-4} mol) and DMSO (5 mL) were placed in a Schlenk tube equipped with a magnetic stirrer bar. The reaction mixture was purged with argon for 20 min, then heated at 65^{o}C for 18 hours. The reaction mixture was cooled, diluted with DCM and washed 3-times with brine. The DCM layers were dried over anhydrous $MgSO_4$, filtered and reduced in volume by rotary evaporation. The polymer was recovered by precipitation into petroleum ether, followed by filtration and drying under vacuum for 24 h at 25 °C.

The conversion was 76 % as determined from ^{1}H NMR spectroscopy. The amount of styrene in the resulting copolymer ***P(NIPAM$_{30}$-co-STY$_{2.50}$)-SC(=S)SC$_4$H$_9$ – MacroCTA2*** ($M_{n,SEC}$= 3700, PDI = 1.09, $M_{n,NMR}$ = 3900) was found to be 8 %, which is correlating to 1 STY unit per 12 NIPAM units.

(iii) Cleavage of RAFT end group from the P(NIPAM-co-STY)-SC(=S)SC$_4$H$_9$ MacroCTAs

The purpose of this procedure is to determine the effect of the RAFT end-group on the LCST. 0.10 g of the MacroCTA and 0.12 g Vazo88 were dissolved in DMSO (5 mL) and placed in a Schlenk tube equipped with a magnetic stirrer bar. The mixture was purged with argon for 20 min and then heated at 100 °C for 16 h until the polymer peak at 310 nm, attributed to the -SC(=S)SC$_4$H$_9$ chromophore, was no longer detected by SEC-PDA. The solution was cooled, diluted with DCM and washed 3-times with brine. The dichloromethane layers were then dried over anhydrous $MgSO_4$, filtered and reduced in volume by rotary evaporation. The polymer was recovered by precipitation into petroleum ether, filtered and dried under vacuum for 24 h at 25 °C.

Two polymers were synthesized as described: *P(NIPAM$_{32}$-co-STY$_{1.33}$)* and *P(NIPAM$_{30}$-co-STY$_{2.50}$)*

RAFT-mediated polymerization of styrene with P(NIPAM-co-STY)-SC(=S)SC$_4$H$_9$ MacroCTAs in water.

A typical polymerisation is as follows: P(NIPAM$_{32}$-*co*-STY$_{1.33}$)-SC(=S)SC$_4$H$_9$ (0.350 g, 5 wt %), SDS (0.0151 g, 5.24 x 10^{-5} mol, < CMC of 8.6 x 10^{-3} M) and MilliQ water (6.25 g) were added to a 10 mL Schlenk tube equipped with magnetic stirrer bar. The polymer was brought down below its LCST by placing the reaction solution in an ice bath to dissolve the

polymer. The solution was then purged with argon for 40 min. A mixture of styrene (0.350 g, 3.4 x 10^{-3} mol, 5 wt %) and AIBN (0.0022 g, 1.34 x 10^{-5} mol, 0.03 wt %) was added with stirring, to facilitate emulsion formation, to the cooled polymer solution. The mixture was purged with argon for another 10 min. The polymerization was commenced by heating the reaction tube in an oil bath at 70 °C. Samples were taken at regular intervals for determination of monomer conversion, molecular weight, molecular weight distribution and particle size.

The polymerisations were carried out for the following MacroCTA /styrene wt% ratios: 5/5 (0.350 g MacroCTA, 0.350 g STY), 5/10 (0.350 g MacroCTA, 0.700 g STY), 10/5 (0.700 g MacroCTA, 0.350 g STY) and 10/10 (0.700 g MacroCTA, 0.700 g STY). In all cases, the amounts of water (6.25 g), SDS (0.0151 g) and AIBN (~0.03 wt % of MacroCTA) were kept constant.

Methods

Determination of Polymer Conversion

Polymer conversion (i.e. copolymerisation of styrene with the MacroCTA) was monitored gravimetrically. Samples (0.4-0.5 mL) were taken at 30 min intervals during polymerisation of up to 3 hours. Collected samples were immediately transferred to pre-weighed aluminium tart pans and their weights (pan and sample) recorded without delay. The weights of pan and sample were again taken after drying under vacuum for at least 12 hours at 25 °C. Polymer conversion was calculated based on the mass loss between the sample droplet and the dried sample and taking into account the mass fraction of water and styrene in the polymerisation mixture. Polymer conversion was also measure by ^{1}H NMR.

Molecular Weight Measurements

Polystyrene-based molecular weights were measured by Size Exclusion Chromatography using a Waters Alliance 2690 Separations Module equipped with an auto-sampler, Differential Refractive Index (RI) detector and a Photo Diode Array (PDA) detector connected in series. HPLC grade tetrahydrofuran was used as eluent at flow rate 1 mL/min. The columns consisted of two 7.8 x 300 mm Waters linear Ultrastyragel SEC columns connected in series.

Particle Size Measurements

Particle size were measured by Dynamic Light Scattering (DLS) technique using a Malvern Zetasizer 3000HS. The sample refractive index (RI) was set at 1.59 for polystyrene. The dispersant viscosity and RI were set to 0.89 and 0.89 Ns/m^2, respectively. Samples for particle size measurements were collected at regular intervals during polymerisation using a syringe attached to a 21-gauge 18mm needle. Four drops of the droplet were mixed with 2.5 mL of MilliQ water pre-heated and kept at 70 °C. The number-average particle diameter of all polymer samples was measured at 70 °C.

Lower Critical Solution Temperature (LCST) Measurements

The LCST of polymers was measured by DLS using a Malvern Zetasizer 3000HS and the same parameters as for the particle size measurements (sample RI = 1.59, dispersant viscosity and RI = 0.89 and 0.89 Ns/m^2, respectively). Approximately 1 mg of the polymer was dissolved in 1 mL of cooled (< 20 °C) MilliQ water. The number-average particle diameters of the polymers were measured at regular intervals from 16 °C to 40 °C.

Nuclear Magnetic Resonance (NMR) Spectroscopy

All NMR spectra were recorded on a Bruker DRX 500 MHz spectrometer using an external lock ($CDCl_3$) and utilizing the solvent peak as an internal reference.

Transmission Electron Microscopy (TEM)

The polymer latex samples were analysed using a JEOL-1010 transmission electron microscope set to an accelerating voltage of 80 kV with spot size 6 at ambient temperature. A typical TEM grid preparation was as follows: A polymerization mixture after the cooling process was diluted with MilliQ water to a concentration of approximately 0.05 wt%. A 10 μL aliquot of the solution was then allowed to air dry onto a formvar precoated copper TEM grid.

Temperature directed morphology transformation (TDMT) method after the RAFT-mediated emulsion polymerizations

(i) Cooling from 70 – 25 °C without adding toluene

After a reaction time of 3 h, the reaction vessel at 70 °C was opened, the latex exposed to air and maintained under these conditions for 4 h. This procedure resulted in loss of most if not all unpolymerized styrene from the latex without a change in the molecular weight distribution.[31] A 0.5 mL aliquot of that polymer latex was then transferred into a preheated (70 °C) glass vial and then cooled rapidly (for 5 min) to 25 ^{o}C.

(ii) Cooling from 70 – 25 °C with adding toluene

After a reaction time of 3 h, the reaction vessel at 70 °C was opened, the latex exposed to air and maintained under these conditions for 4 h to remove unpolymerized styrene (see (i)). A 0.5 mL aliquot of that polymer latex was then transferred into a preheated (70 °C) glass vial containing a specific amount (e.g. 10 μL) of toluene. The glass vial was sealed, shaken

and then rapidly cooled (for 5 min) to 25 ^{o}C. The amounts of toluene used in these experiments were 10 μL and 40 μL.

(iii) Cooling from 70 – 25 ^{o}C under sonication

Immediately after the polymerization, the reaction vessel at 70 ^{o}C was opened (exposing the latex to air) and maintained under these conditions for 4 h to remove unpolymerized styrene (see (i)). A 0.5 mL aliquot of this latex was then transferred to a vial at 70 ^{o}C containing 10 μL of toluene. The vial was sealed, shaken and placed in an Elmasonic S10(H) (Elma GmbH & Co KG) ultrasound bath (at a frequency of 37 kHz) at 65 ^{o}C for 30 min, and then cooled under sonication to 25 ^{o}C over 1 h. The cooling process was aided through the addition of ice over time.

RESULTS AND DISCUSSION

Two MacroCTAs were synthesized using the RAFT technique. The first, MacroCTA1, was synthesized from the solution copolymerization of NIPAM (97.5 mol% in the feed) and styrene (2.5 mol% in the feed) at 65 ^{o}C for 18 h. Conversion and the number-average molecular weight ($M_{n,NMR}$) determined by ^{1}H NMR was 76% and 4000, respectively, and on average gave 1.33 styrene and 32 NIPAM units per chain (i.e. P(NIPAM$_{32}$-co-STY$_{1.33}$)-SC(=S)SC$_4$H$_9$). The $M_{n,SEC}$ and dispersity (Đ) found by SEC was 3800 and 1.07, respectively, suggesting excellent control of the MWD. Polymerization with a higher feed of styrene resulted in the formation of MacroCTA2, in which the $M_{n,NMR}$ (=3900) and $M_{n,SEC}$ (=3700) was similar to that of MacroCTA1 with a low Đ (1.09). The copolymer composition of MacroCTA2 was on average found to have 2.5 units of styrene and 30 units of NIPAM (i.e. P(NIPAM$_{30}$-co-STY$_{2.5}$)-SC(=S)SC$_4$H$_9$). Both MacroCTAs were purposely synthesized to have similar molecular weight and number of NIPAM units. The only measurable difference

between the MacroCTAs was the number of copolymerized styrene units, which for MacroCTA2 was nearly double that of MacroCTA1. The LCSTs of the MacroCTAs with and without the RAFT end-group (i.e. $–SC(=S)C_4H_9$) are given in Figure 1. For both MacroCTAs with the RAFT end-group, the start of aggregation or onset of the LCST occurred at a lower temperature with a broad transition upon further heating. In comparison, the MacroCTAs without RAFT showed a higher initial temperature for the onset of the LCST and a sharper transition with increased temperature. Based on the data in Figure 1, we chose to cool the latex from 70 to 25 ^{o}C to undergo the TDMT process.

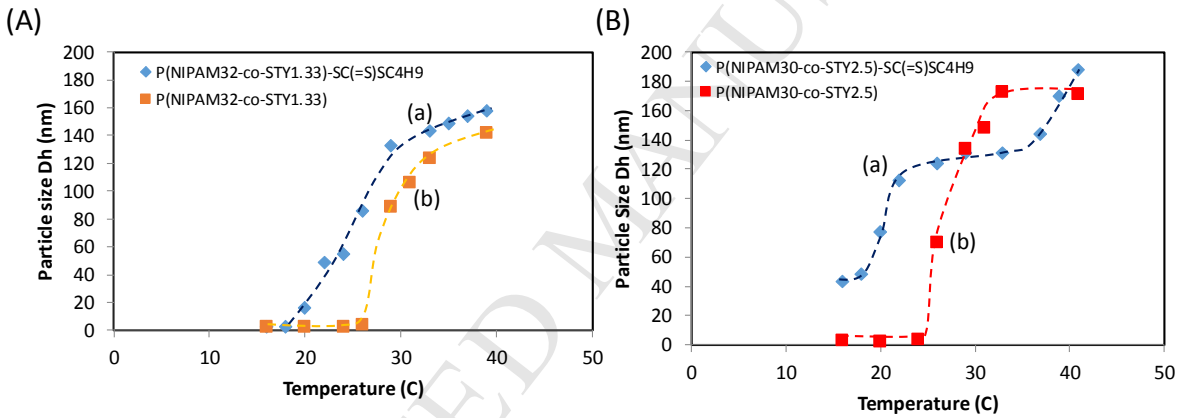

Figure 1. Dynamic light scattering (DLS) of MacroCTAs in water with temperature. (A) MacroCTA1 ($P(NIPAM_{32}$-*co*-$STY_{1.33})$-$SC(=S)SC_4H_9$): (a) with RAFT end-group, (b) without RAFT end-group. (B) MacroCTA2 ($P(NIPAM_{30}$-*co*-$STY_{2.50})$-$SC(=S)SC_4H_9$): (a) with RAFT end-group, (b) without RAFT end-group.

The RAFT-mediated emulsion polymerization of styrene using the MacroCTAs as seed particles was carried out under various reaction conditions. To stabilize the PNIPAM MacroCTA seed particles when heated in water above its LCST, SDS surfactant was added at just below that of the critical micelle concentration (CMC). The absence of SDS micelles will

ensure that the primary locus of polymerization will be within the seed particles. The oil soluble initiator, AIBN, was used to provide the highest possibility for all seed particles to be nucleated at the same time due to its short half-life (~4 h) at 70 ^{o}C.

The first set of emulsions with MacroCTA1 as the seed particles used different ratios of MacroCTA1 to styrene (see Table 1). For Rxn 1 ((MacroCTA:STY = 5:5 wt%), conversion reached 74% after 180 min (curve a in Figure 2A). Increasing the MacroCTA:STY to 10:5 wt% (curve b, Rxn 2) resulted in a significant increase in the rate of polymerization reaching 86% conversion in 90 min. When the styrene ratio was increased to 10 wt% at either 5 (Rxn 3) or 10 wt% (Rxn 4) of MacroCTA there was a drastic retardation in the rate of polymerization, in which conversion reached a plateau of ~30% after 90 min with no further increase in conversion even after long polymerization times (curve c and d). In all four polymerizations, the MWD was well controlled with dispersity values at 180 min of less than 1.11; the only exception was Rxn 4 (Đ = 1.17). It was found that the hydrodynamic diameters (D_h) for Rxns 1 to 3 at 180 min were similar (ranging between 156-163 nm), and their PSD were narrow (PDI_{DLS} < 0.1). The particle size remained relatively constant with a narrow PSD over the polymerization, supporting a constant particle number concentration (N_c) over time and suggesting that the main locus of polymerization was within the MacroCTA seed particles with little or no secondary nucleation. In the case of Rxn 4, the particle size was also relatively constant (D_h ~ 200 nm) over conversion but the PSD was relatively broad (PDI_{DLS} = 0.191 at 180 min). This may be a result of particle aggregation rather than secondary particle nucleation.

Table 1. RAFT-mediated emulsion polymerization at 70 °C in water using SDS as surfactant and AIBN as initiator and MacroCTA1 (P(NIPAM$_{32}$-*co*-STY$_{1.33}$)-SC(=S)SC$_4$H$_9$).

Rxn	**MacroCTA1:STY** (wt%)	**Time** (min)	**Conv** (x)	**SEC (Block)**		**DLS**	
				Mn	Đ	Dh (nm)	PDI_{DLS}
1	5:5	15	0.14	4270	1.10	157	0.034
	[MacroCTA]:[AIBN]=6.9	30	0.19	4500	1.10	146	0.067
		60	0.35	5280	1.09	114	0.061
		90	0.57	6330	1.10	155	0.046
		120	0.67	6950	1.10	157	0.058
		150	0.72	7590	1.10	162	0.025
		180	0.74	8020	1.10	156	0.091
2	10:5	15	0.11	3600	1.11	156	0.132
	[MacroCTA]:[AIBN]=7.3	30	0.35	3660	1.11	108	0.163
		60	0.68	3960	1.11	116	0.106
		90	0.86	4690	1.11	158	0.072
		120	0.82	5180	1.11	164	0.053
		150	0.85	5220	1.11	158	0.074
		180	0.78	5230	1.11	163	0.068
3	5:10	13	0.08	4030	1.08	179	0.083
	[MacroCTA]:[AIBN]=6.9	30	0.13	4330	1.08	146	0.070
		60	0.21	4940	1.10	159	0.025
		90	0.30	5650	1.10	142	0.032
		120	0.37	6070	1.11	161	0.035
		150	0.35	6160	1.11	161	0.019
		180	0.35	6160	1.11	159	0.042
4	10:10	15	0.05	3240	1.10	218	0.096
	[MacroCTA]:[AIBN]=8.2	30	0.07	3230	1.10	212	0.173
		60	0.16	3470	1.10	201	0.171
		90	0.30	4100	1.10	185	0.157
		120	0.42	4600	1.14	202	0.110
		150	0.32	5070	1.14	197	0.161
		180	0.30	5660	1.17	213	0.191

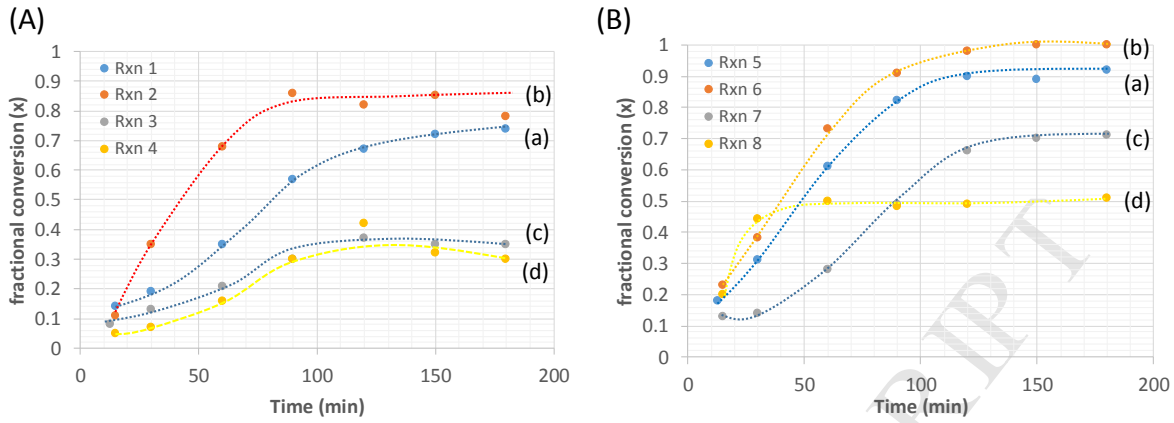

Figure 2. Kinetic for RAFT-mediated emulsion polymerization of styrene initiated with AIBN in water at 70 ^{o}C in the presence of a MacroCTA. (A) MacroCTA1: (a) Rxn 1, (b) Rxn 2, (c) Rxn 3, (d) Rxn 4. (B) MacroCTA2: (a) Rxn 5, (b) Rxn 6, (c) Rxn 7, (d) Rxn 8.

The second set of emulsions using MacroCTA2, consisting of a higher number of styrene units, as the seed particles was carried out at different ratios of MacroCTA2 to styrene (see Table 2). At the lowest ratio (i.e. MacroCTA2:STY = 5:5 wt%), the polymerization was faster than Rxn 1 (i.e. with MacroCTA1) reaching 90% conversion in 90 min (curve a in Figure 2B). An increase in the ratio of MacroCTA to STY (10:5 wt%) led to a slight increase in the polymerization rate compared to Rxns 5 and 2, reaching near complete conversion after 150 min (curve b). Increasing the STY amount to 10 wt% (Rxn 7, curve c) resulted in a decrease in the polymerization rate compared to Rxn 5 and 6, but higher than that for Rxn 3. At a MacroCTA2:STY of 10:10 wt% (Rxn 8, curve d), there was an initial rapid rate of polymerization reaching 44% after 30 min that was similar to the fastest polymerization found (i.e. Rxn 6), but after this time the polymerization virtually stopped with no further conversion observed. The MWD was well controlled for all four polymerizations with narrow MWDs and M_n values close to theory. The values for D_h after 180 min for Rxns 5 to 7 ranged

from 119 to 135 nm with narrow PSD (PDI_{DLS} < 0.1). Similar to Rxn 4, at 10 wt% of both STY and MacroCTA2 (Rxn 8) the size at 180 min was 126 nm but with a broad PSD (PDI_{DLS} > 0.1). In all four polymerizations, the particle size remained relatively constant over time, again supporting that the MacroCTA seed particles was the main locus of polymerization.

Table 2. RAFT-mediated emulsion polymerization at 70 °C in water using SDS as surfactant and AIBN as initiator and MacroCTA2 ($P(NIPAM_{30}$-*co*-$STY_{2.50})$-$SC(=S)SC_4H_9$).

Rxn	**MacroCTA2:STY** (wt%)	**Time** (min)	**Conv** (x)	**SEC (Block)**		**DLS**	
				Mn	Đ	Dh (nm)	PDI_{DLS}
5	5:5	13	0.18	4690	1.06	118	0.045
	[MacroCTA]:[AIBN]=6.9	30	0.31	5210	1.07	98	0.110
		60	0.61	6440	1.07	104	0.076
		90	0.82	7270	1.08	110	0.075
		120	0.90	7570	1.08	122	0.042
		150	0.89	7530	1.08	120	0.063
		180	0.92	7640	1.08	119	0.046
		240	0.92	7650	1.07	121	0.051
6	10:5	15	0.23	3490	1.11	139	0.025
	[MacroCTA]:[AIBN]=7.3	30	0.38	3650	1.13	123	0.061
		60	0.73	4420	1.13	130	0.046
		90	0.91	5170	1.18	130	0.047
		120	0.98	5330	1.13	133	0.046
		150	>0.99	5910	1.21	131	0.065
		180	>0.99	5760	1.11	135	0.040
7	5:10	15	0.13	3810	1.09	127	0.067
	[MacroCTA]:[AIBN]=6.9	30	0.14	4200	1.09	115	0.059
		60	0.28	5380	1.11	121	0.051
		90	0.49	7370	1.15	118	0.048
		120	0.66	9020	1.17	124	0.037
		150	0.70	9800	1.19	126	0.043
		180	0.71	10480	1.19	127	0.042
8	10:10	15	0.20	3540	1.12	131	0.162
	[MacroCTA]:[AIBN]=8.2	30	0.44	4690	1.15	131	0.139
		60	0.50	5400	1.17	121	0.216
		90	0.48	6240	1.18	130	0.202
		120	0.49	6420	1.18	124	0.136
		180	0.51	6450	1.18	126	0.124

At 5wt% STY, the polymerizations were the fastest producing well-defined block copolymers (i.e. M_n's close to theory and narrow MWDs). When MacroCTA1 was increased from 5 (Rxn 1) to 10 wt% (Rxn 2) at 5 wt% STY, the D_h values were similar and the rate increased markedly. This rate increase was due the increase in N_c. The number of STY units (1.33 on average) in MacroCTA1 will allow swelling of the seed particles resulting in not only an increase in the rate of polymerization but nucleation of all particles at a similar time due to the decomposition of AIBN at 70 ^{o}C to generate a narrow PSD. An increase in the number of incorporated STY units on average from 1.33 to 2.5 (i.e. MacroCTA2 used in Rxns 5 and 6) produced a faster rate of polymerization. This was due to a greater amount of swelling of monomer into the seed particles producing the same well-defined polymer and latex particles. It would therefore seem reasonable that by increasing the amount of monomer to 10 wt%, faster polymerization rates would be observed. In fact, there was a significant retardation in the rate for Rxns 3 and 4 using MacroCTA1. A similar but less drastic effect was found when using MacroCTA2 (Rxns 7 and 8). The data suggests that swelling of the particles using MacroCTA1 was less than that for MacroCTA2 seed particles, and the excess monomer not in the seed particles formed into droplets. However, these droplets will coalesce into a thin monomer layer due to the insufficient SDS surfactant concentration used that would otherwise stabilize the droplets. The result of having such a monomer layer is that control of the rate of polymerization will be governed by the rate of monomer diffusion to the locus of polymerization, a slow process for styrene considering its low partition coefficient in water[39]. This would explain the retardation in rate at higher STY amounts.

The TEMs of the latex particles, after removal of residual styrene monomer and when cooled to 25 ^{o}C, showed spherical particles (see TEM micrographs in SI) with similar sizes to that found by DLS for all 8 polymerizations (Rxns 1-8). Using the TDMT method, 0.5 mL of latex solution at 70 ^{o}C was added to a preheated vial at 70 ^{o}C containing 10 μL of toluene

(see Figure 3 and Figures S1-S8 in SI). Toluene was added to reduce the T_g of PSTY to allow transformation for the block copolymers to self-assemble upon the temperature transition from a globule to coil conformation of the PNIPAM block (i.e. decreasing the temperature below the LCST). From Figure 3, the spheres transform towards worms with 10 μL of toluene when the number of STY units in the second block was less than 40 (i.e. Rxns 1, 2 and 4). These worms seemed to be tethered to small spheres to form jelly fish type structures. A similar observation was found for Rxns 6 and 8 in Figure S6 and S8 in SI, respectively. When the number of STY units increased to 52 using MacroCTA1 (Rxn 3), discs and spheres were observed (Figure 3C and Figure S3 in SI). Discs are rarely found, and in our system seem to be kinetically trapped structures (see below). In the case of MacroCTA2 (Rxn 5 with 41 STY units in the second block), the TEMs showed the presence of spheres with protrusions of short worms, whereas for Rxn 7 (with 65 STY units), the predominant structure was spheres with a few number of worms and vesicle-type structures.

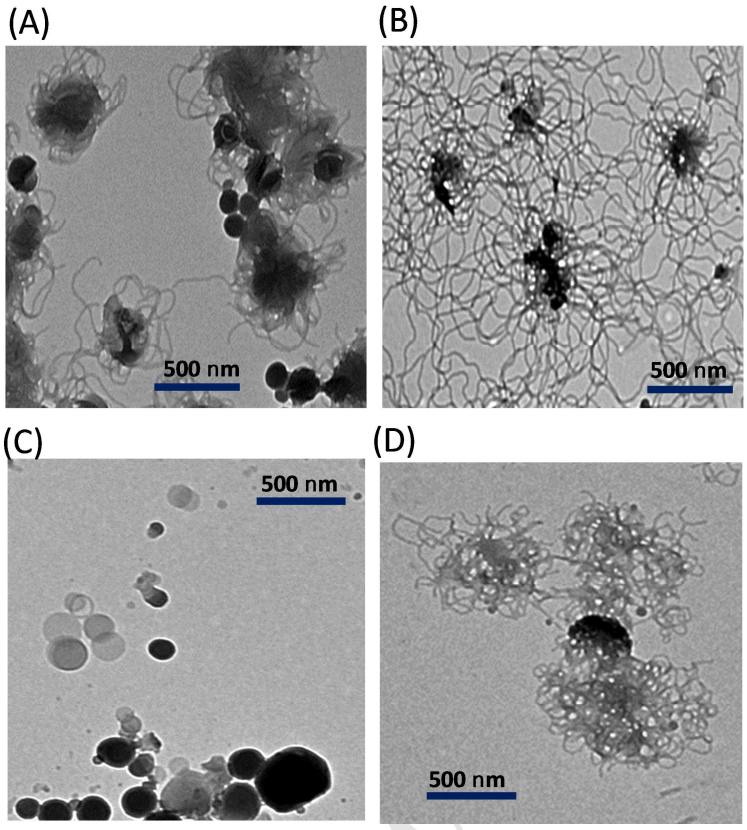

Figure 3. TEM images of the latex nanostructures from RAFT-mediated emulsion polymerization after cooling from 70 to 25 ^{o}C in the presence of 10 μL of toluene. (A) Rxn 1, (B) Rxn 2, (C) Rxn 3, (D) Rxn 4.

An increase to 40 μL of added toluene should provide insight into whether the structures observed at 10 μL were kinetically trapped or close to their thermodynamic equilibrium structure. It can be seen in Figure 4 (for Rxns 1, 2 and 4) that the higher amount of added toluene drove the structures towards worms. Only in Rxn 4 (Figure 4C) did the structures fully converted to worms. The additional toluene for Rxns 1 and 2 further extended the structures towards jelly fish structures with longer cylindrical arms, a similar result also found for Rxns 5, 6 and 8 (see SI). All these reactions consisted of less than 41 STY units in the second block. The disc structure in Rxn 3 (52 STY units in the second block) also seemed

to drive towards jelly fish structures with short cylindrical arms with greater toluene. For Rxn 7 (65 STY units, Figure S7 in SI), the predominant structure was spheres with a few vesicles. All these structures appear consistent with the self-assembly of amphiphilic block copolymers; a greater hydrophobic block produce predominantly spheres, whereas an equal number of hydrophilic to hydrophobic units drives the structures towards cylindrical (worm) structures.[32]

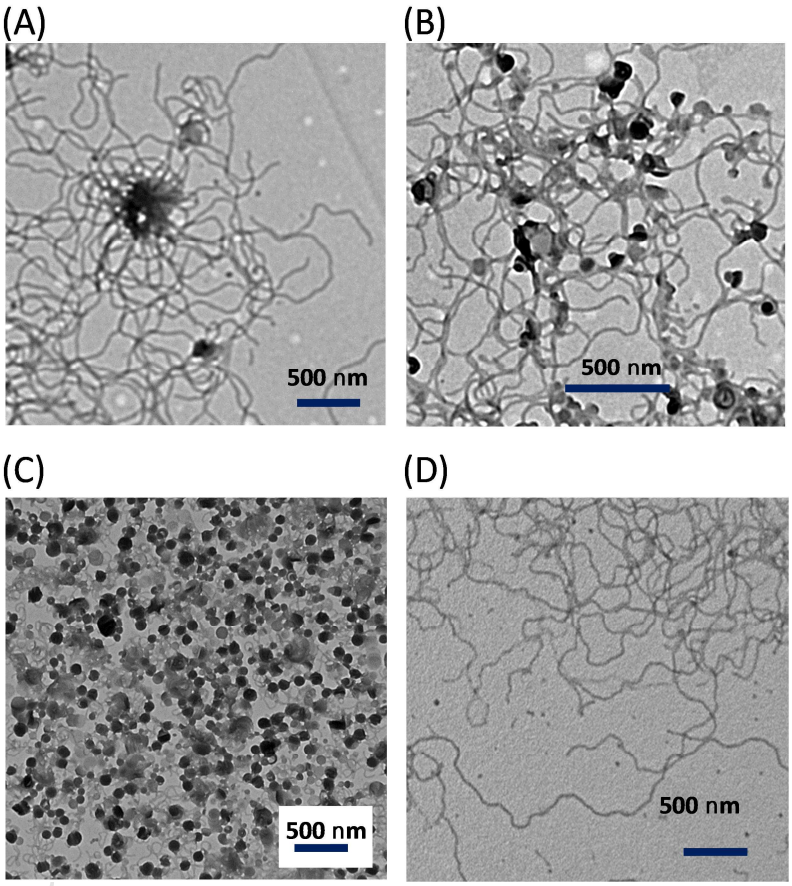

Figure 4. TEM images of the latex nanostructures from RAFT-mediated emulsion polymerization after cooling from 70 to 25 ^{o}C in the presence of 40 μL of toluene. (A) Rxn 1, (B) Rxn 2, (C) Rxn 3, (D) Rxn 4.

Ultrasound provides a mechanical strain on polymers and provides additional energy to mechanically drive self-assembly. Here, we cool the latex to 65 ^{o}C with sonication for 30 min in the presence of 10 μL of toluene, and then the latex was further cooled to 25 ^{o}C under sonication for 1 h. When the number of STY units on the second block was greater than 50 (i.e. Rxns 3 and 7), the TEMs showed spheres (see Figures S7D and 5A). Vesicles were observed for Rxn 5 (41 STY units in the second block, Figure 5B and S5D), and the predominance of a cauliflower structure for Rxn 4 (Figure 5C and S4D). All other reactions consisted of worms and small vesicles (Rxn 2, Figure S2D), small vesicles and jelly fish structures (Rxn 6, Figure S6D), and small vesicles and cauliflower structures (Rxn 8, Figure 8D). We postulate that the difference in structure at 25 ^{o}C between the direct cooling and cooling with sonication was that during sonication, toluene may be removed from the STY core due to the local high energy, thus producing kinetically trapped structures stabilized by the glassy PSTY.

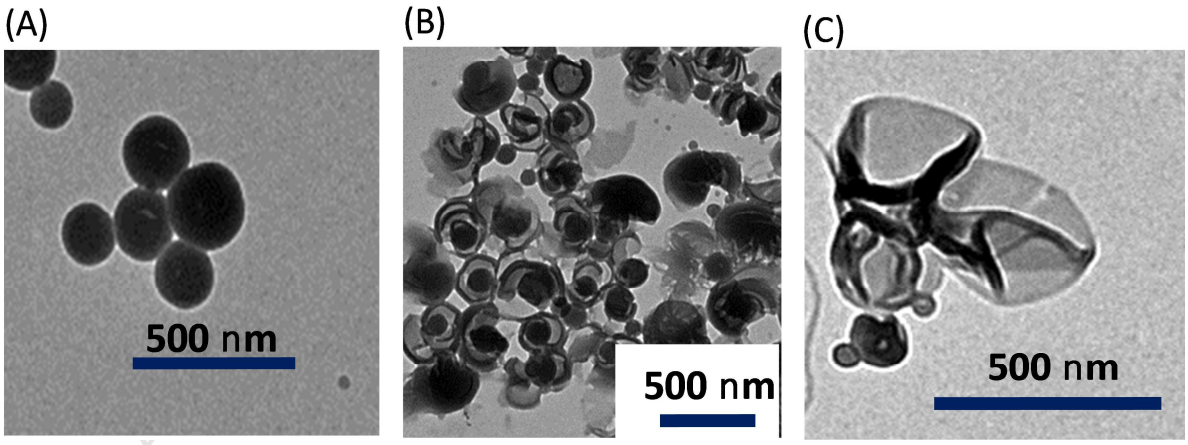

Figure 5. TEM images of the latex nanostructures when the polymerization mixture in the presence of 10 μL of toluene was cooled from 70 to 25 ^{o}C with sonication. (A) Rxn 7, (B) Rxn 5, (C) Rxn 1.

CONCLUSION

In summary, the incorporation of a few styrene units into the PNIPAM MacroCTA allowed these polymer chains, when heated above the MacroCTA, to form seed particles capable of swelling with styrene monomer. The rate of polymerization for the chain extension of the MacroCTA with styrene was fastest when the amount of styrene was 5 wt% and the MacroCTA was 10 wt% due to the increase in particle number. The incorporation of more styrene units in the MacroCTA (i.e. MacroCTA2) gave the fastest rates of polymerization at this styrene amount. Further swelling allowed rapid nucleation of all seed particles as supported by the narrow PSD. In most polymerizations, control of the MWD was excellent with narrow distributions (i.e. Đ <1.11). Retardation and in one case inhibition was found when the styrene amount was increased to 10 wt%. This was most probably due to the limited swelling ability of styrene in the seeds and in combination with the low concentration of stabilizing surfactant, caused the excess monomer to form a monomer layer at the top of the polymerization mixture. This layer controls the rate of polymerization during an interval II system due to the rate of diffusion of monomer from the layer to the growing particles. For the hydrophobic styrene monomer, the rate of diffusion will be slow due to the low partition coefficient of styrene in water. It was found that when these latex particles were cooled to below the LCST of the PNIPAM block in the presence of a small amount of toluene, the spheres transformed into worms, jelly fish and even the rare disc structure. Ultrasound was also used to manipulate the final structure to either vesicles of cauliflowers when cooled in the presence of a small amount of toluene.

Acknowledgment. M.J.M acknowledges financial support from the ARC Discovery grant (DP140103497).

REFERENCES

1. Monteiro, M. J.; Hodgson, M.; De Brouwer, H. J. Polym. Sci., Part A: Polym. Chem. 2000, 38, (21), 3864-3874.

2. Urbani, C. N.; Monteiro, M. J., RAFT-mediated polymerization in heterogeneous systems. In Handbook of RAFT Polymerization, Barner-Kowollik, C., Ed. Wiley-VCH Verlag GmbH & Co. KGaA: 2008; pp 285-314.

3. Monteiro, M. J.; Charleux, B., Living radical polymerisation in emulsion and miniemulsion. . In Chemistry and Technology of Emulsion Polymerisation, Herk, A. v., Ed. Blackwell Publishing Ltd.: 2005; pp 111-139.

4. Zetterlund, P. B.; Kagawa, Y.; Okubo, M. Chem. Rev. 2008, 108, (9), 3747-3794.

5. Cunningham, M. F. Prog. Polym. Sci. 2008, 33, (4), 365-398.

6. McLeary, J. B.; Klumperman, B. Soft Matter 2006, 2, (1), 45-53.

7. Monteiro, M. J. Macromolecules 2010, 43, (3), 1159-1168.

8. Monteiro, M. J.; Cunningham, M. F. Macromolecules 2012, 45, (12), 4939-4957.

9. Monteiro, M. J. J. Polym. Sci., Part A: Polym. Chem. 2005, 43, (15), 3189-3204.

10. Monteiro, M. J. J. Polym. Sci., Part A: Polym. Chem. 2005, 43, (22), 5643-5651.

11. Johnston-Hall, G.; Monteiro, M. J. Macromolecules 2007, 40, (20), 7171-7179.

12. Johnston-Hall, G.; Monteiro, M. J. J. Polym. Sci., Part A: Polym. Chem. 2008, 46, (10), 3155-3173.

13. Luo, Y. W.; Tsavalas, J.; Schork, F. J. Macromolecules 2001, 34, (16), 5501-5507.

14. Ferguson, C. J.; Hughes, R. J.; Nguyen, D.; Pham, B. T. T.; Gilbert, R. G.; Serelis, A. K.; Such, C. H.; Hawkett, B. S. Macromolecules 2005, 38, (6), 2191-2204.

15. Ferguson, C. J.; Hughes, R. J.; Pham, B. T. T.; Hawkett, B. S.; Gilbert, R. G.; Serelis, A. K.; Such, C. H. Macromolecules 2002, 35, (25), 9243-9245.

16. Rieger, J.; Osterwinter, G.; Bui, C. O.; Stoffelbach, F.; Charleux, B. Macromolecules 2009, 42, (15), 5518-5525.

17. Rieger, J.; Stoffelbach, F.; Bui, C.; Alaimo, D.; Jerome, C.; Charleux, B. Macromolecules 2008, 41, (12), 4065-4068.

18. Rieger, J.; Zhang, W. J.; Stoffelbach, F.; Charleux, B. Macromolecules 2010, 43, (15), 6302-6310.

19. de Brouwer, H.; Tsavalas, J. G.; Schork, F. J.; Monteiro, M. J. Macromolecules 2000, 33, (25), 9239-9246.

20. Lansalot, M.; Davis, T. P.; Heuts, J. P. A. Macromolecules 2002, 35, (20), 7582-7591.

21. Tsavalas, J. G.; Schork, F. J.; de Brouwer, H.; Monteiro, M. J. Macromolecules 2001, 34, (12), 3938-3946.

22. Prescott, S. W.; Ballard, M. J.; Rizzardo, E.; Gilbert, R. G. Macromolecules 2002, 35, (14), 5417-5425.

23. Adamy, M.; van Herk, A. M.; Destarac, M.; Monteiro, M. J. Macromolecules 2003, 36, (7), 2293-2301.

24. Monteiro, M. J.; de Barbeyrac, J. Macromolecules 2001, 34, (13), 4416-4423.

25. Monteiro, M. J.; Sjoberg, M.; van der Vlist, J.; Gottgens, C. M. J. Polym. Sci., Part A: Polym. Chem. 2000, 38, (23), 4206-4217.

26. Charmot, D.; Corpart, P.; Michelet, D.; Zard, S. Z.; Biadatti, T. WO 9858974 1998.

27. Bell, C. A.; Smith, S. V.; Whittaker, M. R.; Whittaker, A. K.; Gahan, L. R.; Monteiro, M. J. Adv. Mater. 2006, 18, (5), 582-+.

28. Urbani, C. N.; Monteiro, M. J. Macromolecules 2009, 42, (12), 3884-3886.

29. Sebakhy, K. O.; Kessel, S.; Monteiro, M. J. Macromolecules 2010, 43, (23), 9598-9600.

30. Canning, S. L.; Smith, G. N.; Armes, S. P. Macromolecules 2016, 49, (6), 1985-2001.

31. Kessel, S.; Urbani, C. N.; Monteiro, M. J. Angew. Chem., Int. Ed. 2011, 50, (35), 8082-8085.

32. Kessel, S.; Truong, N. P.; Jia, Z. F.; Monteiro, M. J. J. Polym. Sci., Part A: Polym. Chem. 2012, 50, (23), 4879-4887.

33. Jia, Z.; Truong, N. P.; Monteiro, M. J. Polym. Chem. 2013, 4, (2), 233-236.

34. Jia, Z. F.; Bobrin, V. A.; Truong, N. P.; Gillard, M.; Monteiro, M. J. J. Am. Chem. Soc. 2014, 136, (16), 5824-5827.

35. Bobrin, V. A.; Monteiro, M. J. J. Am. Chem. Soc. 2015, 137, (50), 15652-15655.

36. Tran, N. T. D.; Jia, Z. F.; Truong, N. P.; Cooper, M. A.; Monteiro, M. J. Biomacromolecules 2013, 14, (10), 3463-3471.

37. Tran, N. T. D.; Truong, N. P.; Gu, W.; Jia, Z.; Cooper, M. A.; Monteiro, M. J. Biomacromolecules 2013, 14, (2), 495-502.

38. van Nostrum, C. F.; Veldhuis, T. F. J.; Bos, G. W.; Hennink, W. E. Polymer 2004, 45, (20), 6779-6787.

39. Gilbert, R. G., Emulsion Polymerization. A Mechanistic Approach. 1995.

Graphical Abstract

to

RAFT-Mediated Emulsion polymerization of Styrene with a Thermoresponsive MacroCTA.

*Clovia I. Holdsworth,[2] Zhongfan Jia,[1] and Michael J. Monteiro[1,]**

Highlights

- Heterogeneous RAFT polymerization using a thermoresponsive MacroCTA
- Rapid polymerization and excellent control over MWD with narrow particle size distribution
- Transformation into worms, vesicles, and other unique nanostructures.